Journal of Electromyography and Kinesiology 67 (2022) 102705

Contents lists available at ScienceDirect

Journal of Electromyography and Kinesiology

journal homepage: www.elsevier.com/locate/jelekin

Estimation of contractile parameters of successive twitches in unfused tetanic contractions of single motor units – A proof-of-concept study using ultrafast ultrasound imaging in vivo

Robin Rohlén [a,b,*], Rositsa Raikova [c], Erik Stålberg [d], Christer Grönlund [a]

[a] Department of Radiation Sciences, Radiation Physics, Biomedical Engineering, Umeå University, Umeå, Sweden
[b] Department of Biomedical Engineering, Lund University, Lund, Sweden
[c] Institute of Biophysics and Biomedical Engineering, Bulgarian Academy of Sciences, Sofia, Bulgaria
[d] Department of Clinical Neurophysiology, University Hospital, Uppsala, Sweden

A B S T R A C T

During a voluntary contraction, motor units (MUs) fire a train of action potentials, causing summation of the twitch forces, resulting in fused or unfused tetanus. Twitches have been important in studying whole-muscle contractile properties and differentiation between MU types. However, there are still knowledge gaps concerning the voluntary force generation mechanisms. Current methods rely on the spike-triggered averaging technique, which cannot track changes in successive twitches' properties in response to individual neural firings. This study proposes a method that estimates successive twitches contractile parameters of single MUs during low force voluntary isometric contractions in human biceps brachii. We used a previously developed ultrafast ultrasound imaging method to estimate unfused tetanic activity signals of single MUs. A twitch decomposition model was used to decompose unfused tetanic activity signals into individual twitches. This study found that the contractile parameters varied within and across MUs. There was an association between the inter-spike interval and the contraction time ($r = 0.49, p < 0.001$) and the half-relaxation time ($r = 0.58, p < 0.001$), respectively. The method shows the proof-of-concept to study MU contractile properties of individual twitches in vivo, which can provide further insights into the force generation mechanisms of voluntary contractions and response to individual neural discharges.

1. Introduction

During a voluntary contraction, the fibres of a motor unit (MU) are repeatedly depolarized by neural discharges. Each depolarization causes a twitch and the causing summation of the twitch forces, resulting in a fused or partially fused muscle response (Fuglevand et al., 1993; Grimby et al., 1979). The (partially) fused muscle response depends on the fibres' contractile properties and the characteristics of the neural discharges (Heckman and Enoka, 2004). Therefore, twitches have been important in studying whole muscle contractile properties (Bélanger and McComas, 1985; Milner-Brown et al., 1973, 1974) and differentiation between fast and slow MU types (Sica and McComas, 1971), but there are still knowledge gaps concerning the force generation mechanisms related to increased activity (e.g., training) or decreased activity (e.g., ageing processed) (Celichowski et al., 2014).

The most common method to measure twitches involves simultaneously measuring joint force signals with a single MU trigger based on either electro-stimulated time instants or neural discharge times of single MU in voluntary contractions. The contractile properties of MU twitches can then be estimated using spike-triggered averaging (Negro et al., 2014), providing average twitch estimates. This technique provides a selective summation of the muscle twitch attributable to that MU (Milner-Brown et al., 1973; Monster and Chan, 1977; Stephens and Usherwood, 1977; Thomas et al., 1997). In contrast to measuring force signals that provide the sum of twitch forces of all active MUs, the twitch has also been studied through the diffusion of water molecules through the membrane during electro-stimulated contractions using magnetic resonance imaging (Heskamp et al., 2021). Another approach to studying the twitch is through the MU fibre's thickening and corresponding radial displacement (Macgregor et al., 2018), which is the approach that ultrafast ultrasound imaging (UUS) has considered (Deffieux et al., 2008; Rohlén et al., 2020a). The UUS imaging technique provides the explicit mechanical dynamics of the contracting muscle tissue and allows studying the activity of single MUs in a large field of view. These imaging techniques have been used to study contractile parameters of twitches using electro-stimulation and spike-triggered averaging. Although the spike-triggered averaging technique has provided mechanical insights, it results in biased twitch estimates (Calancie and Bawa, 1986; Gossen et al., 2003; Nordstrom et al., 1989; Taylor et al., 2002) that extract the characteristics of the unfused force transient

* Corresponding author.
E-mail address: robin.rohlen@umu.se (R. Rohlén).

https://doi.org/10.1016/j.jelekin.2022.102705
Received 11 May 2022; Received in revised form 6 September 2022; Accepted 13 September 2022
Available online 17 September 2022
1050-6411/© 2022 The Authors. Published by Elsevier Ltd. This is an open access article under the CC BY license (http://creativecommons.org/licenses/by/4.0/).

instead of the individual twitches (Lim et al., 1995). In addition, spike-triggered averaging requires a high number of firings to provide an average twitch with a high signal-to-noise ratio (Lubel et al., 2022). Therefore, it cannot be used to track changes in the twitch properties in short time intervals or changes in response to individual neural discharges.

Changes in muscle's mechanical properties due to a previous discharge have been studied using electro-stimulation (Kamavuako and Farina, 2010). The contractile parameters of the twitches have been shown to vary because of so-called slack and calcium build-up mechanisms (Kamavuako and Farina, 2010). A method to study individual successive twitches of a single MU has been proposed using decomposition of its unfused tetanic activity by mathematical modelling using a peel-off approach (Raikova et al., 2008, 2007). This technique has been applied to electro-stimulated isometric contractions with constant and varying stimuli in the rodent model by measuring the unfused tetanic activity using a force transducer (Celichowski, 1992; Celichowski et al., 2005; Raikova et al., 2007). For example, it has been shown that the preceding inter-spike interval (ISI) can predict the twitch contraction time at varying ISI (Krutki et al., 2008; Piotr et al., 2012). However, no study has explored *individual twitches* and their variation during *voluntary* human contractions in vivo. The analysis of voluntarily generated individual twitches in vivo may provide valuable physiological insights into health and disease. The possible explanation for the lack of studies related to voluntary individual MU twitches may be that it is difficult to acquire information on the unfused tetanic activity of *single MUs* in voluntary contractions. A method to solve this limitation was recently demonstrated: an MU ultrafast ultrasound (MU-UUS) analysis was proposed to identify unfused tetanic contraction dynamics of single MUs during voluntary isometric contractions (Rohlén et al., 2020b, 2020a).

This study proposes a method to estimate contractile parameters of successive twitches of single MUs during voluntary contractions using the recently proposed MU-UUS analysis (Rohlén et al., 2020b, 2020a). We applied a previously validated spatiotemporal decomposition approach of ultrafast ultrasound sequences to find independent components in agreement with single MU needle EMG activity. Afterwards, we implemented a twitch decomposition model on the identified components. Finally, the contractile parameters of detected twitches were presented and compared against the inter-spike intervals from the EMG. Experiments on healthy subjects' biceps brachii under low force isometric contractions were obtained using synchronised measurements from UUS imaging and concentric needle electromyography (nEMG). First, we quantified the variability of the contractile parameters within a MU. Then, we analysed their relationship to the preceding inter-spike interval (ISI) with the hypothesis that the twitches vary from one discharge to another, closely related to the ISI. Finally, we performed a sensitivity analysis to test the robustness of the results.

2. Methods

2.1. Assumptions and terminology

This study observed the twitches by radial displacement of single MUs (Fig. 1). Each muscle fibre bundle belonging to a MU is shortening and transversely linked to *radial displacement* (Baskin and Paolini, 1967). In Fig. 1, ten neural spikes (discharges) resulted in a force output and a radial displacement output, a relationship that has shown to be highly correlated (Sato et al., 2022; Yoshitake et al., 2008). So, if the muscle volume remains constant during compression (Ophir et al., 1999) and the force is proportional to the stretch (Hill, 1938), small changes in force are approximately linear with the radius change (Fig. S1, Supplementary material). Although the axial velocity may also be sensitive to the contribution of fibres moving up or downward with respect to the probe, the assumption that those movements are the sum of successive twitches remains valid.

The radial displacement output is (defined as) the sum of successive twitches denoted as unfused tetanic activity (UTA). That means that the UTA comprises ten individual twitches shifted in time and the summation of the individual twitches reconstructs the UTA. So, an individual twitch is the radial displacement caused by a given neural spike that reconstructs the UTA with the other individual twitches.

2.2. Overview

The following analysis pipeline extracted the contractile parameters of successive twitches of contracting single MU during isometric contractions through four steps (Fig. 2). 1) Acquisition of contraction tissue dynamics using UUS from a cross-section of biceps brachii with nEMG as a reference for single MU activity. 2) Estimation of unfused tetanic activity (UTA) of single MUs using the MU-UUS (Rohlén et al., 2020a) method. 3) Selection of the highest quality single MUs UTA using nEMG spike train. 4) Estimating contractile parameters of the single MUs UTA using a decomposition method (Raikova et al., 2008). The primary analysis was then to estimate the variability of successive twitch parameters and their association with ISI. Finally, sensitivity analysis on the successive twitches' contractile parameters and their association to ISI was conducted by variations of steps 2, 3 and 4 in Fig. 2.

2.3. Experimental protocol

Simultaneous UUS and nEMG were acquired from the biceps brachii muscle in nine healthy subjects (33 ± 7 years old, four men and five

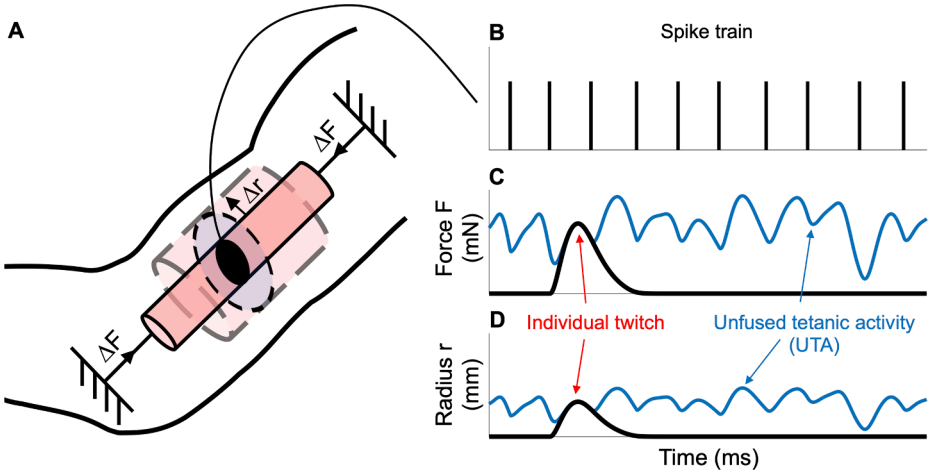

Fig. 1. A. Observing unfused tetanus through the radial displacement of (the muscle fibre bundle of) single motor units (MUs). Each muscle fibre bundle is shortening and transversely linked to radial displacement. **B.** Ten neural spikes (discharges, black vertical lines) resulted in (**C**) a force output based on the force change (ΔF) and (**D**) a radial displacement output and radius change (Δr). The radial displacement output is the sum of successive twitches denoted as unfused tetanic activity (UTA). That means that the UTA comprises ten individual twitches shifted in time which summation reconstructs the UTA. So, an individual twitch is the radial displacement caused by a given neural spike that reconstructs the UTA with the other individual twitches.

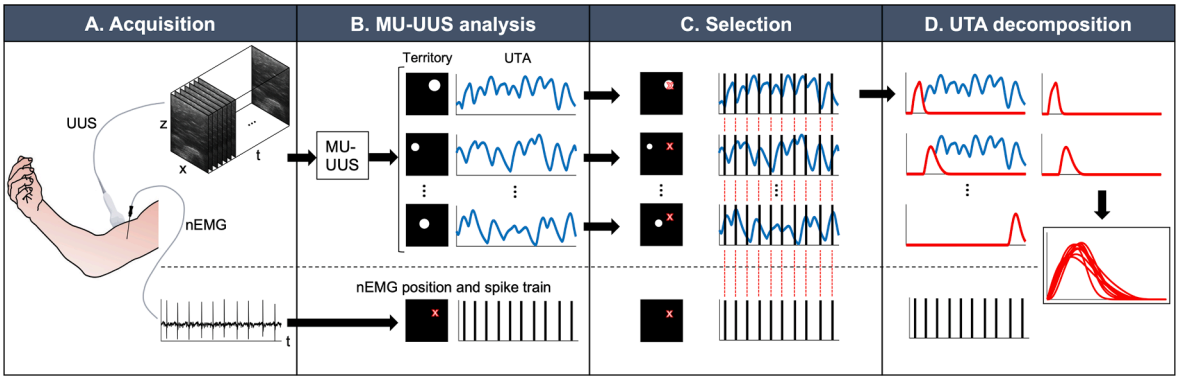

Fig. 2. A. Tissue contraction dynamics were acquired using ultrafast ultrasound (UUS) signal from a cross-section of biceps brachii with concentric needle electromyography (nEMG) acquired simultaneously as a reference. **B.** An MU-UUS analysis method estimated unfused tetanic activity (UTA) for single motor units (MUs). **C.** The selection of single MUs UTA using simultaneously sampled nEMG spike train. **D.** The estimation of contractile parameters of the single MUs UTA using a decomposition method. Finally, sensitivity analyses were conducted by considering variations of steps **B**, **C**, and **D**.

women) who performed weak isometric voluntary contractions by elbow flexion and supination of their lower arm. A physician inserted a concentric needle into the biceps brachii muscle, and each subject performed low force isometric elbow flexion (90 degrees). The subjects received feedback regarding the degree of activation from a loudspeaker displaying the EMG sound, and the physician adjusted the needle within the muscle to obtain clear EMG activity of a single MU. This procedure is according to a standard clinical routine where physicians extract MU characteristics for diagnosing neuromuscular diseases. When clear EMG activity was obtained, the ultrasound probe was positioned proximal to needle insertion such that the image plane captured the needle tip (Fig. 2A). From the nine healthy subjects, 64 synchronised measurements that were two seconds long were collected. The UUS and nEMG systems were synchronized using a customized synchronization procedure (Rohlén et al., 2020a). The subjects gave informed consent before the experimental procedure. The project conformed to the Declaration of Helsinki and was approved by the Swedish Ethical Review Authority (2019–01843).

The UUS recordings were performed on an Ultrasonix SonixTouch (Ultrasonix Medical Corporation, Richmond, CA), a 9 MHz L9-4 linear transducer, and a 128 channel DAQ module. The data was recorded using a plane wave transmit and parallel receive sequence at 2000 images per second (Bercoff, 2011). The radiofrequency data was sampled with a field of view of 40x40 mm at 40 MHz and reconstructed using the sum-and-delay beamforming method (Deffieux et al., 2008). The reconstructed radiofrequency data provided the basis for calculating the axial tissue velocity image sequences (Loupas et al., 1995) with a range gate length of 1 mm and an ensemble length of 10 ms. The reconstructed radio frequency signals were band-pass filtered (2–15 MHz Butterworth with order 6), and the velocity data were high pass filtered in the time dimension (5 Hz Butterworth with order 6).

The nEMG recordings were performed on a Cadwell Sierra Wave EMG machine (Cadwell Laboratories Inc., Kennewick, WA, USA) with a 38x0.45 mm concentric needle electrode (AMBU® Neuroline, DEN). After removing a low-frequency synchronisation signal effect, the spike trains were estimated (Stålberg et al., 1995) and manually double-checked.

2.4. MU-UUS analysis – Estimation of single MU UTA

Single MU UTAs were estimated using the MU-UUS method (Rohlén et al., 2020a) (Fig. 2B). In short, the method works as follows: a sub-region of 20x20 mm is shifted with jumps of five millimetres laterally and vertically in the velocity images, resulting in 25 sub-regions. Next, each sub-region is split into 25 spatiotemporal components using spatiotemporal independent component analysis (stICA) (Stone et al., 2002). Each component has a spatial map and a time signal. This procedure results in 625 components from each recording (25 components in every 25 sub-regions), where each component has a spatial map and a temporal signal (Fig. 2B). Finally, each component's spike train was estimated based on the local maxima of the temporal signal after band-pass filtering (Rohlén et al., 2020b, 2020a, 2022a).

The component's temporal signal from the MU-UUS analysis is the estimated UTA in terms of velocity. The following three steps obtained the resulting estimation of single MU UTAs in terms of displacement: 1) filtering using a fourth-order Butterworth high-pass filter at 5 Hz with zero-phase distortion, 2) rectangular (numerical) integration, and 3) adjustment by a vertical shift such that all points in the signal have non-negative values. The vertical shift was motivated because the experimental procedure was set up such that the ultrasound recording started after contraction onset, i.e., we did not measure the initial first twitches' build-up of the unfused tetanic activity of the steady isometric contraction. Instead, we started the ultrasound recording once a MU was stable in terms of the loudspeaker feedback for the EMG activity. By then, many twitches had already occurred since the resting state. Therefore, velocity signal integration in the middle of a contraction may be negative at some point, depending on the characteristics of the neural firings and the corresponding twitches.

2.4.1. Selection of UTA of single MUs using nEMG spike train as reference

The selection of UTAs belonging to a single MU was based on computing the rate of agreement (RoA) metric (Fig. 2C). RoA quantifies the spike train similarities by $\text{RoA} = 100 \times c_j/(c_j + A_j + B_j)$, where c_j is the number of spikes of the j^{th} spike train that was identified, A_j is the number of false identified spikes, and B_j is the number of unmatched spikes. We set the tolerance interval for the RoA metric to be 30 ms, motivated by the electro-mechanical delay (Begovic et al., 2014), meaning that each spike of a component needs to be within 30 ms of the spike from nEMG to be considered a match. As in a previous study (Rohlén et al., 2020a), we selected only one component based on the maximal RoA (out of the 625 components), although we observed the same 'physical' component across the 625 components multiple times due to overlap of the different 20x20 mm region-of-interest (ROI) windows. The selection of MU UTA was based on those components with RoA $\geq$ 90%, which were the values that were considered successful in other studies using the RoA metric (Holobar et al., 2010; Negro et al., 2016).

2.5. Estimation of successive twitches and their contractile parameters

Estimation of twitches and their contractile parameters based on the UTA is performed by a six-parameter twitch model (6PTM) that is well-

documented and validated by the decomposition of UTA in rats (Celichowski et al., 2014; Raikova et al., 2018, 2016, 2010, 2008, 2007). The general concept of the 6PTM is that six parameters can model each twitch. These parameters are the lead time T_{lead}, the half-contraction time T_{hc}, the contraction time T_c, the half-relaxation time T_{hr}, the duration of the twitch T_{tw}, and the maximal displacement D_{max}. The analytical equations are presented in Raikova et al. (2008), and the parameters are illustrated in Fig. 3.

Briefly, 6PTM consists of the following steps. First, the initial twitch is evaluated, and the six parameters are calculated such that the residual between the modelled twitch and the first experimental twitch of UTA is minimized. This modelled twitch is subtracted from the UTA, and if the tetanus is unfused enough, the second twitch is visible. Next, the second twitch is modelled in the same way by calculating the six parameters. The first and the second modelled twitches are subtracted from the UTA. This process is repeated until the last twitch. A summary of the decomposition procedure is illustrated in Fig. 2D.

There was a large variation in the twitches' amplitude due to the ambiguity in the stICA algorithm (Hyvärinen et al., 2001) used within the MU-UUS analysis (Rohlén et al., 2020a). Due to the twitches' amplitude ambiguity, it was standardized (zero mean and unit variance) for each set of parameters in each UTA before assessment.

2.6. Sensitivity analyses

Three sensitivity analyses were applied to test the robustness of the results and the method's validity. Since this is the first time this method has been applied to UTA signals of tissue velocity (and not force twitch signals), it is unknown how their presumable lower signal-to-noise ratio affects its performance. Therefore, we performed an inter-observer analysis where two independent observers decomposed each UTA to evaluate the robustness of the decomposition method (Fig. 2D). The adjusted MU-UUS analysis replaced the stICA method to test the potential influence on the UTA estimation (Rohlén et al., 2020a). The stICA method splits the sub-regions into 25 spatiotemporal components, and it was replaced by stSOBI (Theis et al., 2005) (with a focus only on spatial dimension), which has been shown to provide a similar rate of agreement with the EMG reference as stICA (Rohlén et al., 2022b). Third, the selection of included data was broadened, including all UTA with RoA $\geq$ 70%, motivated by mean RoA in MU identifications from Rohlén et al. (2020) (Fig. 2C).

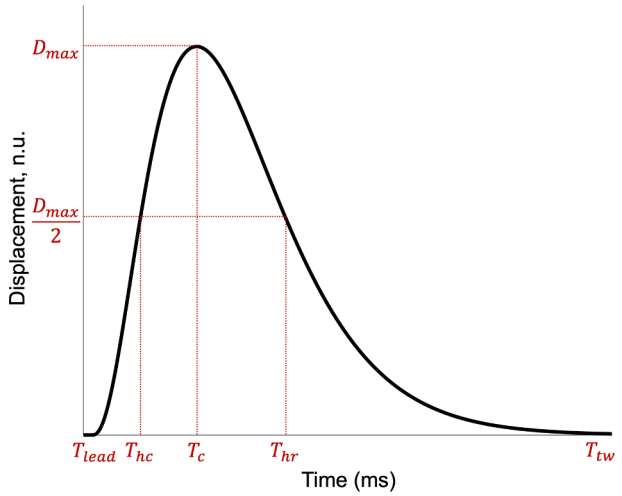

Fig. 3. The six-parameter twitch model (6PTM). The six parameters (red colour) are the following: T_{lead} – lead time; D_{max} – maximal displacement (amplitude); T_c – the time when the maximal amplitude is reached; T_{hc} – time where during increasing the phase of the contraction the half of D_{max} is reached; T_{hr} – the time when during relaxation phase the half of maximal amplitude is reached; T_{tw} – the duration of the twitch.

2.7. Statistical analysis

Descriptive statistics of the contractile parameters were quantified using the mean and standard deviations. Linear regression models quantified linear relationships between the different contractile parameters (dependent variable) and the preceding ISI (independent variable). Testing reliability was performed using the intraclass correlation coefficient (ICC) (McGraw and Wong, 1996). A p-value of 0.05 was set for statistical significance.

3. Results

3.1. Variation of contractile parameters of successive twitches

Based on RoA $\geq$ 90%, the UTA selection resulted in n = 7 UTAs from four subjects, and 146 individual twitches were extracted. The descriptive statistics of the estimated contraction time (T_c) and the half-relaxation time (T_{hr}) are summarized in Table 1. For all parameters, see

Table 1
A summary of the individual twitches' contractile parameters for all MUs.

		Quality	*Intervallength*	*Contractile parameters*		*Model fit*
MU #	**MU Index**	**RoA (%)**	**ISI (ms)**	**T_c (ms)**	**T_{hr} (ms)**	***r***
Primary analysis						
#14	**1**	100	96 (13)	59.8 (8.5)	102.5 (10.5)	0.94
#3	**2**	96	65 (6)	47.9 (10.2)	85.8 (13.9)	0.91
#4	**3**	96	71 (10)	38.6 (8.5)	68.2 (11.4)	0.99
#7	**4**	94	101 (13)	59.4 (9.0)	105.1 (10.5)	0.96
#11	**5**	94	100 (15)	50.6 (8.2)	96.3 (7.9)	0.94
#6	**6**	93	66 (6)	41.2 (7.5)	69.2 (10.9)	0.87
#5	**7**	92	68 (6)	43.0 (9.3)	76.5 (12.2)	0.99
Mean	**1–7**	**95.0**	**81**	**47.5**	**83.7**	**0.94**
Std	**1–7**	**2.6**	**17**	**11.5**	**17.9**	**0.04**
CV	**1–7**	**2.8**	**21**	**24.3**	**21.4**	**4.6**
Sensitivity analysis						
#2	**8**	83	109 (10)	58.2 (18.3)	98.1 (17.6)	0.92
#13	**9**	81	93 (8)	49.1 (14.1)	85.2 (14.5)	0.89
#9	**10**	80	93 (10)	52.8 (12.2)	98.4 (16.3)	0.87
#10	**11**	80	89 (10)	52.5 (12.4)	93.8 (15.7)	0.95
#1	**12**	78	116 (14)	47.5 (12.4)	89.7 (15.8)	0.80
#12	**13**	71	114 (22)	51.7 (13.3)	96.9 (15.9)	0.89
#8	**14**	70	111 (9)	50.2 (15.0)	90.1 (12.5)	0.73
Mean	**8–14**	**77.6**	**104**	**51.8**	**93.2**	**0.86**
Std	**8–14**	**5.1**	**11**	**14.0**	**15.9**	**0.08**
CV	**8–14**	**6.5**	**11**	**27.0**	**17.0**	**8.7**
Mean	**All**	**86.3**	**92**	**49.3**	**87.7**	**0.90**
Std	**All**	**9.8**	**18**	**12.8**	**17.7**	**0.07**
CV	**All**	**11.4**	**20**	**25.9**	**20.1**	**7.8**

The values are presented as the mean with standard deviation in parenthesis for the interval length and the contractile parameters. The model fit relates to the six-parameter twitch against the experimental UTA. The presented parameters are based on the decomposition of the first operator. ISI = inter-spike interval, MU = motor unit, std = standard deviation, RoA = rate of agreement (nEMG-UUS), CV = coefficient of variation (%), r = Pearson's linear correlation coefficient, nEMG = concentric needle-electromyography, UUS = ultrafast ultrasound. T_c = contraction time (ms), T_{hr} = half-relaxation time (ms).

Table S1 in the Supplementary material. The correlation (r) between experimental UTA and the model fit was 0.94 ± 0.04 (see Fig. 4). The ISI of the MUs ranged from 65 to 101 ms (9.9 Hz to 15.3 Hz), and the ISI had a standard deviation between 6 and 22 ms (Table 1). The lead time (T_{lead}), the half-contraction time (T_{hc}), the contraction time (T_c), the half-relaxation time (T_{hr}), and the duration of the twitch (T_{tw}) were 7.4 ± 3.5 ms, 18.4 ± 4.8 ms, 47.5 ± 11.5 ms, 83.7 ± 17.9 ms, and 183.7 ± 36.7 ms, respectively.

3.1.1. Association between contractile parameters and inter-spike interval (ISI)

The ISI was significantly associated with contraction time T_c (r = 0.49, $p < 0.001$) and half-relaxation time T_{hr} (r = 0.58, $p < 0.001$) (Fig. 5). The ISI was also significantly associated with T_{lead}, T_{hc}, and T_{tw}, but the relationship was weaker ($r = 0.33$, $r = 0.30$, $r = 0.46$; $p < 0.001$) (Fig. S2, Supplementary material). The ISI was not associated with the (normalized) displacement (R^2 = 0.00, p = 0.064) (Fig. S2, Supplementary material). The linear relationships of ISI and the contractile parameters on a single MU-level did not show any associations with the ISI, suggesting that the average ISI for each MU is causing this association across all MUs (Fig. 5).

3.2. Sensitivity analyses

First, the inter-observer analysis of estimated contractile parameters (T_{lead}, T_{hc}, T_c, T_{hr}, T_{tw}, D_{max}) was reliable in terms of absolute agreement (ICC) across the four subjects and the 146 twitches (ICC = 0.94 ± 0.04; $p < 0.001$) resulting in a similar linear relationship between ISI and the contraction time T_c (r = 0.49 and r = 0.46; $p < 0.001$) and half-relaxation time T_{hr} ($r = 0.58$ and $r = 0.61$, $p < 0.001$) (Fig. 6A-B).

Second, reproducibility using two different decomposition methods (stICA, stSOBI) in the MU-UUS method was good (Cicchetti and Sparrow, 1981) for parameters T_{hc}, T_c, T_{hr}, and T_{tw} (ICC = 0.67 ± 0.05; $p <$ 0.001). The results of the linear associations between ISI and contractile parameters were similar to the primary analysis. There was a significant linear relationship between ISI and the contraction time T_c ($r = 0.61$, $p < 0.001$) and half-relaxation time T_{hr} ($r = 0.71$, $p < 0.001$) (Fig. 6C-D).

Third, the selection of UTA based on RoA ≥ 70% resulted in n = 14 from seven subjects, i.e., seven more UTAs from three additional subjects. The descriptive statistics of the estimated contractile parameters are summarized in Table 1. The model fit was similar to the primary analysis (0.90 ± 0.07). The contractile parameters were within the margin of error compared to the primary analysis (Table 1). The association between ISI and the contractile parameters was similar but slightly weaker than the primary analysis. There was a significant association between ISI and contraction time T_c ($r = 0.35$, $p < 0.001$) and between ISI and the half-relaxation time T_{hr} (r = 0.48, $p < 0.001$) (Fig. 6E-F).

4. Discussion

This work aimed to estimate individual twitch parameters from single MUs and analyse the successive twitch variability during voluntary low force isometric contractions recorded by UUS imaging. The main finding is that 1) the contractile parameters of individual twitches varied, and 2) there was a positive association between the ISI and the contraction and half-relaxation time across the MUs.

4.1. The absolute value of contraction parameters

The estimated contraction and half-relaxation time variables (47.5 ± 11.5 and 83.7 ± 17.9 ms) were lower than in two previous studies on biceps brachii using UUS and electro-stimulation. The first study on three healthy subjects reported contraction and half-relaxation times to be 1) 66.3 ± 5.7 and 102.9 ± 11.0 ms, 2) 70.0 ± 2.3 and 104.0 ± 12.5 ms, and 3) 73.4 ± 8.6 and 114.5 ± 24.0 ms (Deffieux et al., 2008). The second study, also on three healthy subjects, reported similar contraction and half-relaxation times as the first: 1) 72 ± 14 and 104 ± 28 ms, 2) 57 ± 16 and 113 ± 39 ms, and 3) 69 ± 25 and 101 ± 51 ms (Grönlund et al., 2013). However, both studies used electro-stimulation with a frequency well below the firing rates of the MUs in this study. Since we found that a lower firing rate was associated with a larger contraction and half-relaxation time, this could explain their larger values. This study included many MUs with a 14–15 Hz firing rate, which may result in shorter contractions than those with a lower firing rate. Considering some of the MUs with lower firing rates, e.g., MU #7 and MU #14, which had a firing rate of 9.9 and 10.4 Hz and their average contraction and half-relaxation times were 1) 59.4 ± 9.0 ms and 105.1 ± 10.5 ms, and 2) 59.8 ± 8.5 ms and 102.5 ± 10.5 ms. So, these values were similar to the previously reported values. In addition, other imaging techniques, such as MU magnetic resonance imaging (Heskamp et al., 2021), have reported contraction times on the gastrocnemius and soleus muscles, similar to those reported by Deffieux et al. (2008). Other studies using non-imaging techniques support the contraction times in this study. For example, Yoshitake et al. (2002) used mechanomyography and reported an average contraction of 62.9 ± 4.2 ms (and half-relaxation time 124.1 ± 9.1 ms) from the medial gastrocnemius muscle (Yoshitake et al., 2002). In contrast, the imaging techniques and mechanomyography that consider radial displacement, Bélanger and McComas (1985) used strain gauges to measure torques during elbow flexion. They reported an average contraction time of 70.3 ± 13.5 ms from the biceps brachii of 24 subjects but suggested that the experimental procedure may have slightly prolonged the contraction times.

The lead time (T_{lead}) and the twitch duration (T_{tw}) were difficult to

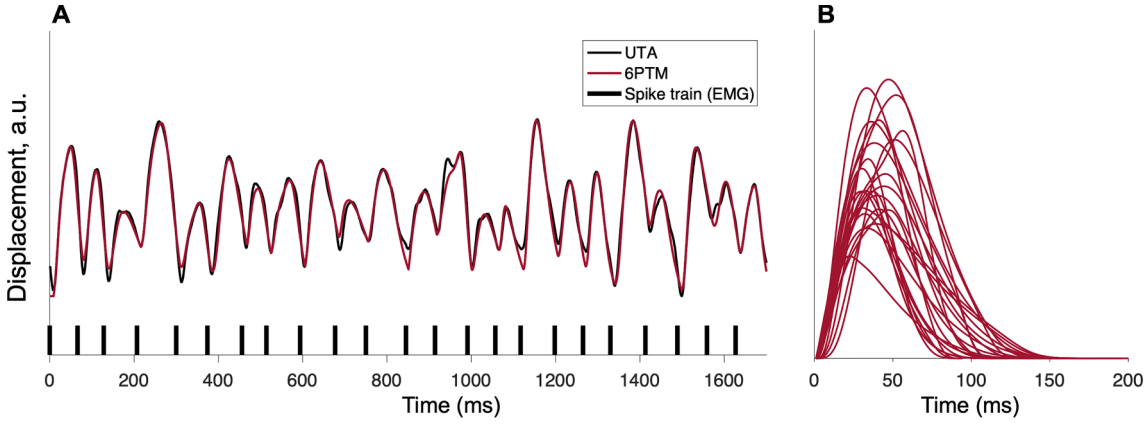

Fig. 4. Modelling a motor unit's unfused tetanic activity (UTA) using the six-parameter twitch model (6PTM). **A.** The experimental UTA (black line) and the modelled UTA (red line). The modelled UTA sums every individual twitch using the EMG spike train (vertical black line). **B.** The decomposed individual twitches.

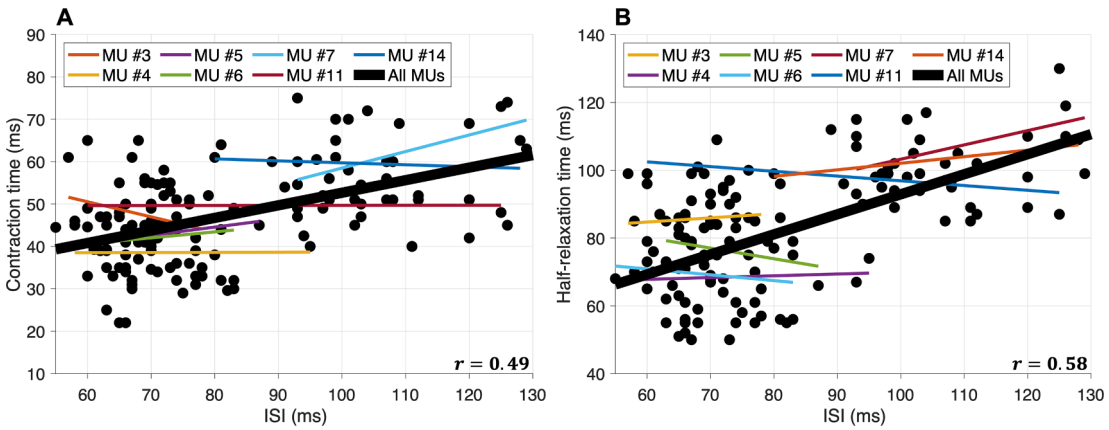

Fig. 5. The inter-spike interval (ISI) was associated with single motor unit (MU) twitches' contractile parameters. **A.** The contraction time T_c were associated with the ISI across all MUs (black line). The linear relationships within the single MUs (coloured lines) did not show any associations with the ISI, suggesting that the average ISI for each MU is causing this association across all MUs. **B.** The half-relaxation time T_{hr} was associated with the ISI across all MUs (black line). Similar to the contraction time, the linear relationships within the single MUs (coloured lines) did not show any associations with the ISI. r denotes the correlation coefficient.

estimate for both operators because the lead time is short, and noise may affect the moment of the start of the contraction. In contrast, the duration of the twitch is often multiple times longer than the ISI and, therefore, usually not visible. The estimated (absolute) contractile parameters based on the MU-UUS analysis have not been validated yet. Consequently, we cannot determine if our slightly lower estimated parameter values are correct. However, the relative variation of the individual twitches of the estimated UTA, and their contraction parameters, showed to be robust since the sensitivity analysis with different decomposition algorithms (stSOBI vs stICA) showed similar results in terms of parameter values and their association with ISI. Therefore, we believe that the estimated twitch contraction parameters were robust and reliable (Fig. 6 and Table 1).

4.2. Variability and ISI association

We found that ISI was significantly associated with the individual twitches' contraction time and half-relaxation time (Fig. 5), e.g., an increasing ISI resulted in longer contraction times. Previous findings using irregular electro-stimulation in the rodent model also showed that ISI was associated with the contraction time (Krutki et al., 2008; Piotr et al., 2012), with a correlation of 0.74, slightly higher than the correlation in this paper (Fig. 6). In Fig. 5, the R^2 is about 24% and 34% and in, e.g., Fig. 6D, the R^2 is about 37% and 50%. These correlations suggest that other physiological factors (and non-physiological factors) should be involved in explaining this linear relationship. In our study, the ISI was associated with contractile parameters on the group level but not for the individual UTAs of single MUs (Fig. 5 and Fig. S2, Supplementary material). Since the contractions were at very low force levels, the active MUs should be slow MUs (type I) and have similar fibre diameters. Therefore, the observed variations in mechanical properties should not be associated with MU characteristics such as size and type. Moreover, we observed firing rates between 8 and 16 Hz. For these reasons, we believe the association is driven by the differences in average ISI of the included UTAs. These potential explanations could be investigated in the future using rat models with functionally isolated MUs (Drzymała-Celichowska and Celichowski, 2020).

The relationship between ISI and the contraction time could be explained by the calcium release mechanism from the sarcoplasmic reticulum. Previously it has been demonstrated that the twitch force of subsequent stimuli increases due to the higher concentration of calcium (Duchateau and Hainaut, 1986a, 1986b), which is the summation of the residual calcium (released on the first neural spike) and the newly released calcium (of the second neural spike) (Hill, 1949). These findings are based on early twitches within a contraction. However, our data are from the stabilized part of unfused tetanus (not observing the first twitches) described in the experimental procedure. According to Henneman's size principle, since the subjects recruited MUs during very low force, these are likely slow MUs (Henneman, 1957; Henneman et al., 1965). There are reports that rats' contractile parameters for electro-stimulated slow MUs converge around the 8th successive twitch if ISI is constant and a 15 Hz stimulus is applied (Raikova et al., 2008). Therefore, the positive linear relationship between ISI and contraction time in this study may be explained by the increased or decreased rate of calcium release from the sarcoplasmic reticulum resulting in a faster or slower contraction. Given this, the proposed method may be used to study the muscle's membrane properties in vivo during voluntary contractions and improve the understanding of force generation mechanisms. Given this, the proposed method shows the proof-of-concept to study MU contractile properties of individual twitches in vivo, which could be used to gain further insights into the mechanisms of force generation of unfused tetanic contractions in response to individual neural discharges during voluntary contractions.

4.3. Limitations

There was a large drop-out (N = 7 and four subjects out of N = 64 and nine subjects) in the selection step, which has been reported and extensively discussed previously (Rohlén et al., 2020a). In the present work, we applied sensitivity analyses to assess the influence on the results caused by this large drop-out. In short, the potential explanations for the drop-out are: 1) A possible inter-subject difference in the mechanical properties of the perimysium (fascicle level) of the skeletal muscle fascia (Blottner et al., 2019; Purslow, 2010). 2) The MU-UUS analysis and the RoA metric rely on the assumption of linearly superpositioned components. However, this is a feasible assumption at low force levels. 3) The concentric needle-EMG may act as a mechanical bridge between the investigated muscle segment, its adjacent muscle tissue, and the penetrated skin and cause an attenuation of the UTA of a MU. The last point could potentially be overcome by integrating high-density surface EMG recordings and UUS (Carbonaro et al., 2022; Lubel et al., 2022). In addition, Carbonaro et al. (2022), using a similar method, considered experimental data up to 10% MVC and 20% MVC for simulated data suggesting feasibility for higher force levels.

The summation of the modelled twitches (modelled UTA) had almost a perfect fit to experimental data within the primary analysis (very high correlation values, Table 1). However, some modelled UTA did not fit well, possibly explained by other physiological activities intermingled in the experimental UTA, such as the activity of other MUs. This explanation suggests that the original MU-UUS method (Rohlén et al., 2020a,

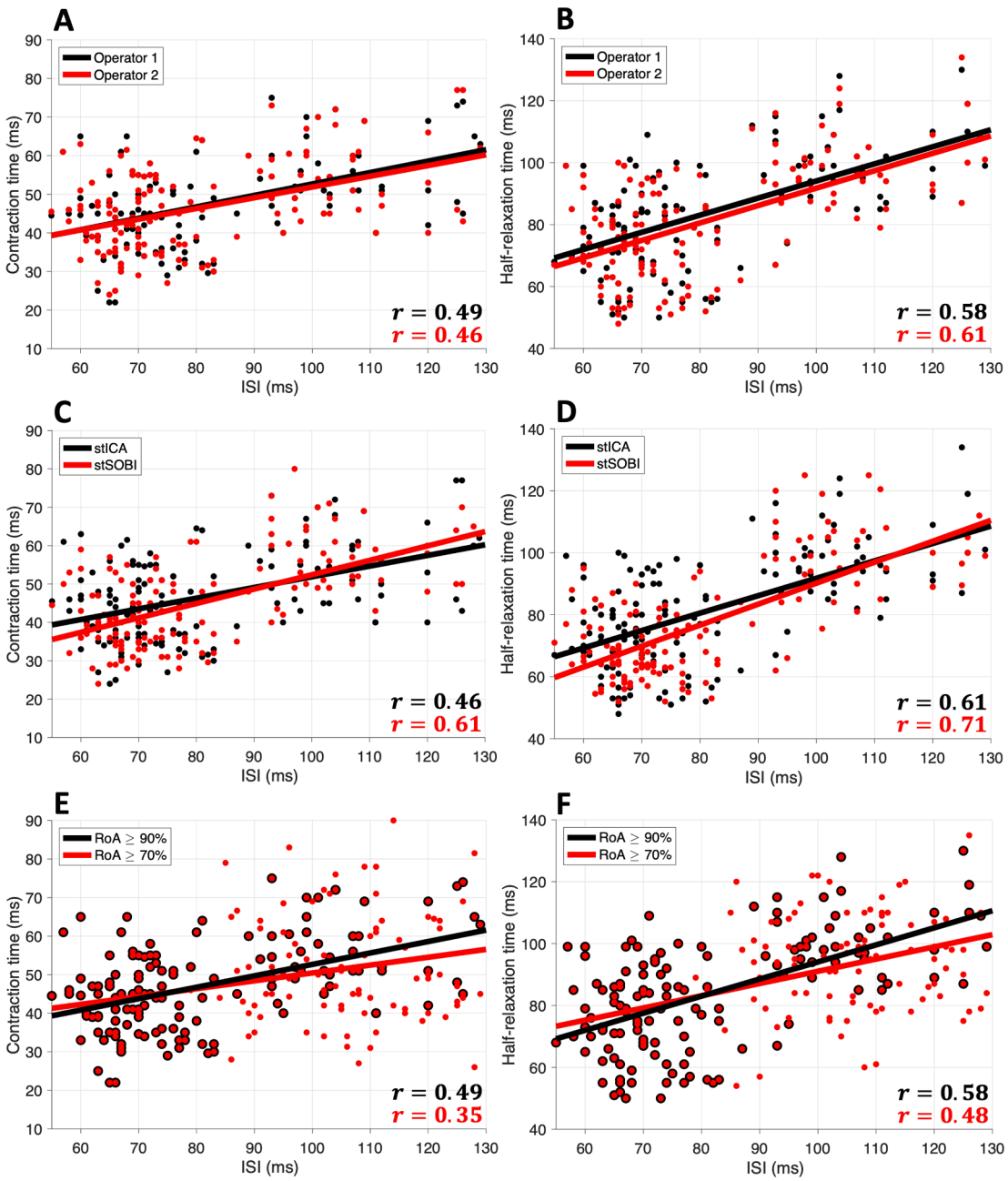

Fig. 6. Sensitivity analyses for testing the robustness of the results. **A-B.** Using two independent operators, the decomposition of UTA had an intraclass correlation coefficient (ICC) of 0.94 ± 0.04, which reflects the similar linear relationships between ISI and contraction time and half-relaxation times for both operators. **C-D.** Testing the reliability of UTA estimation using the MU-UUS method by replacing the existing module (spatiotemporal independent component analysis, stICA) with spatiotemporal second-order blind identification (stSOBI). The ICC for the contractile parameters was 0.67 ± 0.05, and both operators' linear relationships between ISI and half-relaxation time were highly similar. **E-F.** A broader selection criterion (RoA ≥ 70%) resulted in a slightly weaker linear relationship (than the primary analysis) between ISI and the contraction and the half-relaxation time. *r* denotes the correlation coefficient.

b) cannot always fully isolate the single MUs from other muscle-related activities and could be due to the simple cost functions used in the blind source separation module. However, the sensitivity analysis concerning replacing stICA with stSOBI showed that the UTA estimation was reliable (ICC = 0.63).

We observed the twitch inside the muscle at the level of the bundle of contracting muscle fibres of single MUs. We estimated the UTA displacement of single MUs using the MU-UUS method, previously validated using needle-EMG measurements (Rohlén et al., 2020a). While the 6PTM is designed for decomposing force signals into individual twitches, we assume that there is a monotonic relation between the force and the displacement of the contracting MU. We assume that if the muscle volume remains constant during compression and the force is proportional to the stretch, small changes in force are approximately linear to the radius change (Fig. S1, Supplementary material). This assumption may not suit muscle fibres with fibre tapering, but that type of morphology is commonly found in fast-twitch fibres (Monti et al., 2001). Since this study considered very low force levels (about 1% of maximum voluntary contraction), the recruited MUs should be slow ones according to Henneman's size principle (Henneman, 1957; Henneman et al., 1965). Therefore, we believe that this should not have influenced the results.

5. Conclusions

For the first time, this paper estimated successive twitches in unfused tetanic low force voluntary isometric contractions in human biceps brachii. In addition, we found a variation in the contractile parameters of successive twitches and a positive association between the ISI and contraction time and half-relaxation time. The method shows the proof-of-concept to study MU contractile properties of individual twitches in vivo, which can provide further insights into the force generation mechanisms of voluntary contractions and response to individual neural discharges.

Declaration of Competing Interest

The authors declare that they have no known competing financial interests or personal relationships that could have appeared to influence the work reported in this paper.

Acknowledgements

This work was supported by the Swedish Research Council [grant number 2015-04461]; and the Kempe Foundations [grant number JCK-1115].

Appendix A. Supplementary material

Supplementary data to this article can be found online at https://doi.org/10.1016/j.jelekin.2022.102705.

References

Baskin, R.J., Paolini, P.J., 1967. Volume change and pressure development in muscle during contraction. Am. J. Physiol. Content 213 (4), 1025–1030.
Begovic, H., Zhou, G.-Q., Li, T., Wang, Y., Zheng, Y.-P., 2014. Detection of the electromechanical delay and its components during voluntary isometric contraction of the quadriceps femoris muscle. Front. Physiol. 5, 494. https://doi.org/10.3389/fphys.2014.00494.
Bélanger, A.Y., McComas, A.J., 1985. A comparison of contractile properties in human arm and leg muscles. Eur. J. Appl. Physiol. Occup. Physiol. 54 (3), 326–330.
Bercoff, J., 2011. Ultrafast Ultrasound Imaging, In: Minin, I.V., Minin, O.V. (Eds.), Ultrasound Imaging. IntechOpen, Rijeka. doi: 10.5772/19729.
Blottner, D., Huang, Y., Trautmann, G., Sun, L., 2019. The fascia: Continuum linking bone and myofascial bag for global and local body movement control on Earth and in Space. A scoping review. REACH 14–15, 100030. https://doi.org/10.1016/j.reach.2019.100030.
Calancie, B., Bawa, P., 1986. Limitations of the spike-triggered averaging technique. muscle Nerve Off. J. Am. Assoc. Electrodiagn. Med. 9 (1), 78–83.
Carbonaro, M., Meiburger, K.M., Seoni, S., Hodson-Tole, E.F., Vieira, T., Botter, A., 2022. Physical and electrophysiological motor unit characteristics are revealed with simultaneous high-density electromyography and ultrafast ultrasound imaging. Sci. Rep. 12, 1–14.
Celichowski, J., 1992. Motor units of medial gastrocnemius muscle in the rat during the fatigue test. I. time course of unfused tetanus. Acta Neurobiol. Exp 52, 17–21.
Celichowski, J., Pogrzebna, M., Raikova, R.T., 2005. Analysis of the unfused tetanus course in fast motor units of the rat medial gastrocnemius muscle. Arch. Ital. Biol. 143, 51–63.
Celichowski, J., Raikova, R., Aladjov, H., Krutki, P., 2014. Dynamic changes of twitchlike responses to successive stimuli studied by decomposition of motor unit tetanic contractions in rat medial gastrocnemius. J. Neurophysiol. 112 (12), 3116–3124.
Cicchetti, D.V., Sparrow, S.A., 1981. Developing criteria for establishing interrater reliability of specific items: applications to assessment of adaptive behavior. Am. J. Ment, Defic.
Deffieux, T., Gennisson, J.-l., Tanter, M., Fink, M., 2008. Assessment of the mechanical properties of the musculoskeletal system using 2-D and 3-D very high frame rate ultrasound. IEEE Trans. Ultrason. Ferroelectr. Freq. Control 55 (10), 2177–2190.
Drzymała-Celichowska, H., Celichowski, J., 2020. Functional isolation of single motor units of rat medial gastrocnemius muscle. JoVE (Journal Vis, Exp, p. e61614.
Duchateau, J., Hainaut, K., 1986a. Nonlinear summation of contractions in striated muscle. I. Twitch potentiation in human muscle. J. Muscle Res. Cell Motil. 7 (1), 11–17.
Duchateau, J., Hainaut, K., 1986b. Nonlinear summation of contractions in striated muscle. II. potentiation of intracellular Ca 2+ movements in single barnacle muscle fibres. J. Muscle Res. Cell Motil. 7 (1), 18–24.
Fuglevand, A.J., Winter, D.A., Patla, A.E., 1993. Models of recruitment and rate coding organization in motor-unit pools. J. Neurophysiol. 70 (6), 2470–2488.
Gossen, E.R., Ivanova, T.D., Garland, S.J., 2003. Factors affecting the stability of the spike-triggered averaged force in the human first dorsal interosseus muscle. J. Neurosci. Methods 126 (2), 155–164.
Grimby, L., Hannerz, J., Hedman, B., 1979. Contraction time and voluntary discharge properties of individual short toe extensor motor units in man. J. Physiol. 289, 191–201.
Grönlund, C., Claesson, K., Holtermann, A., 2013. Imaging two-dimensional mechanical waves of skeletal muscle contraction. Ultrasound Med. Biol. 39 (2), 360–369.
Heckman, C.J., Enoka, R.M., 2004. Physiology of the motor neuron and the motor unit. Handbook of Clin. Neurophysiol. Elsevier 119–147.
Henneman, E., 1957. Relation between size of neurons and their susceptibility to discharge. Science (80-.) 126 (3287), 1345–1347.
Henneman, E., Somjen, G., Carpenter, D.O., 1965. Functional significance of cell size in spinal motoneurons. J. Neurophysiol. 28 (3), 560–580.
Heskamp, L., Birkbeck, M.G., Whittaker, R.G., Schofield, I.S., Blamire, A.M., 2021. The muscle twitch profile assessed with motor unit magnetic resonance imaging. NMR Biomed. 34, e4466.
Hill, A.V., 1949. The abrupt transition from rest to activity in muscle. Proc. R. Soc. London. Ser. B-Biological Sci. 136, 399–420.
Hill, A.V., 1938. The heat of shortening and the dynamic constants of muscle. Proc. R. Soc. London. Ser. B-Biological Sci. 126, 136–195.
Holobar, A., Minetto, M.A., Botter, A., Negro, F., Farina, D., 2010. Experimental analysis of accuracy in the identification of motor unit spike trains from high-density surface EMG. IEEE Trans. Neural Syst. Rehabil. Eng. 18 (3), 221–229.
Hyvärinen, A., Karhunen, J., Oja, E., Haykin, S. (Eds.), 2001. Adaptive and Learning Systems for Signal Processing, Communications, and ControlIndependent Component Analysis. John Wiley & Sons, Inc., New York, USA.
Kamavuako, E.N., Farina, D., 2010. Time-dependent effects of pre-conditioning activation on muscle fiber conduction velocity and twitch torque. Muscle Nerve 42 (4), 547–555.
Krutki, P., Pogrzebna, M., Drzymała, H., Raikova, R., Celichowski, J., 2008. Force generated by fast motor units of the rat medial gastrocnemius muscle during stimulation with pulses at variable intervals. J. Physiol. Pharmacol. an Off. J. Polish Physiol. Soc. 59, 85–100.
Lim, K.Y., Rymer, W.Z., Thomas, C.K., 1995. Computational methods for improving estimates of motor unit twitch contraction properties. Muscle Nerve Off. J. Am. Assoc. Electrodiagn. Med. 18 (2), 165–174.
Loupas, T., Powers, J.T., Gill, R.W., 1995. An axial velocity estimator for ultrasound blood flow imaging, based on a full evaluation of the Doppler equation by means of a two-dimensional autocorrelation approach. IEEE Trans. Ultrason. Ferroelectr. Freq. Control 42 (4), 672–688.
Lubel, E., Sgambato, B.G., Barsakcioglu, D.Y., Ibáñez, J., Tang, M.-X., Farina, D., 2022. Kinematics of individual muscle units in natural contractions measured in vivo using ultrafast ultrasound. J. Neural Eng.
Macgregor, L.J., Hunter, A.M., Orizio, C., Fairweather, M.M., Ditroilo, M., 2018. Assessment of skeletal muscle contractile properties by radial displacement: the case for tensiomyography. Sport. Med. 48 (7), 1607–1620.
McGraw, K.O., Wong, S.P., 1996. Forming inferences about some intraclass correlation coefficients. Psychol. Methods 1, 30–46.
Milner-Brown, H.S., Stein, R.B., Lee, R.G., 1974. Contractile and electrical properties of human motor units in neuropathies and motor neurone disease. J. Neurol. Neurosurg. Psychiatry 37 (6), 670–676.
Milner-Brown, H.S., Stein, R.B., Yemm, R., 1973. The contractile properties of human motor units during voluntary isometric contractions. J. Physiol. 228, 285–306.
Monster, A.W., Chan, H., 1977. Isometric force production by motor units of extensor digitorum communis muscle in man. J. Neurophysiol. 40 (6), 1432–1443.
Monti, R.J., Roy, R.R., Edgerton, V.R., 2001. Role of motor unit structure in defining function. Muscle Nerve 24, 848–866. https://doi.org/10.1002/mus.1083.
Negro, F., Muceli, S., Castronovo, A.M., Holobar, A., Farina, D., 2016. Multi-channel intramuscular and surface EMG decomposition by convolutive blind source separation. J. Neural Eng. 13, 26027. https://doi.org/10.1088/1741-2560/13/2/026027.
Negro, F., Yavuz, U.Ş., Farina, D., Hug, F., 2014. Limitations of the spike-triggered averaging for estimating motor unit twitch force: a theoretical analysis. PLoS One 9 (3), e92390.
Nordstrom, M.A., Miles, T.S., Veale, J.L., 1989. Effect of motor unit firing pattern on twitches obtained by spike-triggered averaging. Muscle Nerve Off. J. Am. Assoc. Electrodiagn. Med. 12 (7), 556–567.
Ophir, J., Alam, S.K., Garra, B., Kallel, F., Konofagou, E., Krouskop, T., Varghese, T., 1999. Elastography: ultrasonic estimation and imaging of the elastic properties of tissues. Proc. Inst. Mech. Eng. Part H J. Eng. Med. 213 (3), 203–233.
Piotr, K., Jan, C., Rositsa, R., 2012. Motor unit contractions evoked by stimulation with variable interpulse intervals. Biocybern. Biomed. Eng. 32 (3), 29–42.
Purslow, P.P., 2010. Muscle fascia and force transmission. J. Bodyw. Mov. Ther. 14, 411–417. https://doi.org/10.1016/j.jbmt.2010.01.005.
Raikova, R., Celichowski, J., Angelova, S., Krutki, P., 2018. A model of the rat medial gastrocnemius muscle based on inputs to motoneurons and on an algorithm for prediction of the motor unit force. J. Neurophysiol. 120 (4), 1973–1987.
Raikova, R., Celichowski, J., Pogrzebna, M., Aladjov, H., Krutki, P., 2007. Modeling of summation of individual twitches into unfused tetanus for various types of rat motor units. J. Electromyogr. Kinesiol. 17 (2), 121–130.
Raikova, R., Krutki, P., Celichowski, J., Lebedev, M.A., 2016. A general mathematical algorithm for predicting the course of unfused tetanic contractions of motor units in rat muscle. PLoS One 11 (9), e0162385.

Raikova, R., Pogrzebna, M., Drzymała, H., Celichowski, J., Aladjov, H., 2008. Variability of successive contractions subtracted from unfused tetanus of fast and slow motor units. J. Electromyogr. Kinesiol. 18 (5), 741–751.

Raikova, R., Rusev, R., DrzymaŁa-Celichowska, H., Krutki, P., Aladjov, H., Celichowski, J., 2010. Experimentally verified mathematical approach for the prediction of force developed by motor units at variable frequency stimulation patterns. J. Biomech. 43 (8), 1546–1552.

R, Rohlén, C, Antfolk, C, Grönlund, 2022a. Optimization and comparison of two methods for spike train estimation in an unfused tetanic contraction of low threshold motor units. bioRxiv.

Rohlén, R., Stålberg, E., Grönlund, C., 2020a. Identification of single motor units in skeletal muscle under low force isometric voluntary contractions using ultrafast ultrasound. Sci. Rep. 10, 1–11.

Rohlén, R., Stålberg, E., Stöverud, K.H., Yu, J., Grönlund, C., 2020b. A method for identification of mechanical response of motor units in skeletal muscle voluntary contractions using ultrafast ultrasound imaging - simulations and experimental tests. IEEE Access 8, 50299–50311. https://doi.org/10.1109/ACCESS.2020.2980053.

Rohlén, R., Yu, J., Grönlund, C., 2022b. Comparison of decomposition algorithms for identification of single motor units in ultrafast ultrasound image sequences of low force voluntary skeletal muscle contractions. BMC Res. Notes 15, 207. https://doi.org/10.1186/s13104-022-06093-1.

Sato, I., Yamamoto, S., Kakimoto, M., Fujii, M., Honma, K., Kumazaki, S., Matsui, M., Nakayama, H., Kirihara, S., Ran, S., 2022. Basic characteristics between mechanomyogram and muscle force during twitch and tetanic contractions in rat skeletal muscles. J. Electromyogr, Kinesiol, p. 102627.

Sica, R.E.P., McComas, A.J., 1971. Fast and slow twitch units in a human muscle. J. Neurol. Neurosurg. Psychiatry 34, 113–120. https://doi.org/10.1136/jnnp.34.2.113.

Stålberg, E., Falck, B., Sonoo, M., Stålberg, S., Åström, M., 1995. Multi-MUP EMG analysis—a two year experience in daily clinical work. Electroencephalogr. Clin. Neurophysiol. Mot. Control 97, 145–154.

Stephens, J.A., Usherwood, T.P., 1977. The mechanical properties of human motor units with special reference to their fatiguability and recruitment threshold. Brain Res. 125, 91–97.

Stone, J.V., Porrill, J., Porter, N.R., Wilkinson, I.D., 2002. Spatiotemporal independent component analysis of event-related fMRI data using skewed probability density functions. Neuroimage 15, 407–421.

Taylor, A.M., Steege, J.W., Enoka, R.M., 2002. Motor-unit synchronization alters spike-triggered average force in simulated contractions. J. Neurophysiol. 88, 265–276.

F.J, Theis, P, Gruber, I.R, Keck, A.-M, Tomé, E.W, Lang, R.R.R.A, Regensburg, 2005. A spatiotemporal second-order algorithm for fMRI data analysis, in: Proc. CIMED. pp. 194–201.

Thomas, C.K., Broton, J.G., Calancie, B., 1997. Motor unit forces and recruitment patterns after cervical spinal cord injury. muscle Nerve Off. J. Am. Assoc. Electrodiagn. Med. 20, 212–220.

Yoshitake, Y., Masani, K., Shinohara, M., 2008. Laser-detected lateral muscle displacement is correlated with force fluctuations during voluntary contractions in humans. J. Neurosci. Methods 173, 271–278.

Yoshitake, Y., Shinohara, M., Ue, H., Moritani, T., 2002. Characteristics of surface mechanomyogram are dependent on development of fusion of motor units in humans. J. Appl. Physiol. 93, 1744–1752.